

## Noise and Chaos in a Fractal Basin Boundary Regime of a Josephson Junction

M. Iansiti, Qing Hu, R. M. Westervelt, and M. Tinkham

*Physics Department and Division of Applied Sciences, Harvard University, Cambridge, Massachusetts 02138*  
(Received 25 March 1985)

By digital simulations and experiment, we study a Josephson system in a highly nonlinear regime. High experimental noise values appear to correspond in simulations to intrinsic chaotic motion in some regions and to noise-induced hopping between periodic solutions in others. Focusing on the latter, we find correlation between high noise sensitivity and the fractal dimension of the boundary between the basins of the periodic attractors. We show that if enough noise is present to push the orbits into the basin boundary, behavior similar to intrinsic chaos results.

PACS numbers: 74.50.+r, 05.45.+b

The current-biased Josephson junction is a good system for the study of nonlinear dynamics. It can be well represented by the resistively shunted junction (RSJ) model, one of the simplest mathematical systems to show chaotic behavior, well suited to digital and analog simulation. Since the occurrence of these phenomena was first predicted,<sup>1</sup> many reports of different types of chaos in Josephson systems have been made.<sup>2-8</sup> These studies have mostly focused on "intrinsic" chaos, in which the system orbit converges on a strange attractor, causing unpredictably erratic motion. However, Grebogi *et al.*<sup>9</sup> have pointed out the importance of the basins of attraction of a system in determining its dynamics and have shown that their boundaries often have a fractal structure. This causes high sensitivity to initial conditions even if all solutions found are *periodic*. In this work, we present the first study of the effect of noise on a system exhibiting a fractal boundary between basins of periodic attractors, based on extensive simulations and guided by experimental measurement. Our simulations show that the addition of thermal and shot noise appropriate to the experimental situation should induce intermittent motion with excess low-frequency noise output, similar to that expected in an intrinsically chaotic region. This prediction is consistent with our experimental noise measurements.

Our measurements were made on a robust  $5\text{-}\mu\text{m}^2$  Nb-*a*-Si-Nb junction, fabricated at Sperry Research Laboratories by the SNAP process.<sup>10</sup> The junction parameters are  $I_c = 425\ \mu\text{A}$  at 4.2 K,  $R_n = 3.2\ \Omega \sim R_{\text{leak}}/3$ , and  $C = 0.23 \pm 0.01\ \text{pF}$ . The subgap leakage resistance was measured by magnetic depression of the critical current, and the capacitance was chosen to agree with SQUID resonance measurements on larger junctions as described elsewhere.<sup>7</sup> Our ac drive source is an optically pumped far-infrared laser, the output of which is stable to  $\sim 5\%$  during our measurements. The laser radiation is coupled to the junction by means of a half-wave dipole antenna broadly resonant at 400 GHz. Because of its low impedance, the junction is current biased by both the ac and the dc drives, in contrast with previous work done in this frequency range,

in which no chaotic behavior was found.<sup>11</sup>

All digital computer calculations used the current-biased RSJ model, generalized to take account of the change in quasiparticle conductance at the gap voltage by use of a voltage-dependent resistance  $R$ , equal to  $R_n$  above the gap  $[(\Delta_1 + \Delta_2)/e]$  and to  $R_{\text{leak}}$  below the gap. The basic equation is

$$\frac{d^2\phi}{dt^2} + \frac{1}{\beta^{1/2}} \frac{d\phi}{dt} + \sin\phi = i_{\text{dc}} + i_L \sin\left[\frac{\omega_L}{\omega_p} t\right] + i_N, \quad (1)$$

where  $i_{\text{dc}}$ ,  $i_L$ , and  $i_N$  are, respectively, the dc, the laser, and the noise currents, all normalized to the critical current of the junction. Moreover,  $\beta = 2eI_c R^2 C / \hbar \sim 3.3$  for voltages above the gap and  $\sim 28$  below the gap. All times are measured in units of the inverse of the plasma frequency,  $\omega_p = (2eI_c / \hbar C)^{1/2}$ . The laser drive frequency  $f_L = \omega_L / 2\pi = 419\ \text{GHz} \sim 1.1\omega_p / 2\pi$ . Equation (1) was solved with a fourth-order Runge-Kutta algorithm, in double-precision arithmetic.

Experimental measurements (mainly at  $T = 4.2\ \text{K}$ ) and simulations were performed over a wide range of laser and dc currents, with  $0 < i_L < 2.3$  and  $0 < i_{\text{dc}} < 1.5$ . First, simulated and experimental  $I$ - $V$  curves were compared to ensure that satisfactory agreement was reached. The results are impressive, both in the specific features of the  $I$ - $V$  curves, as shown by (a) and (b) in Fig. 1 for a typical value of  $i_L$ , and in the overall quantitative dependence of the critical current on the laser power, shown in Fig. 1(c). The latter fit determines the constant of proportionality between the square root of the measured far-infrared laser power and the induced ac current through the junction, there being no other free parameter. The good agreement depends on the good parameter characterization of the sample and the use of a nonlinear resistance in the simulations. Our main sources of error are the uncertainty in the sample's capacitance value, laser power calibration and fluctuations, and the oversimplification in the piecewise-

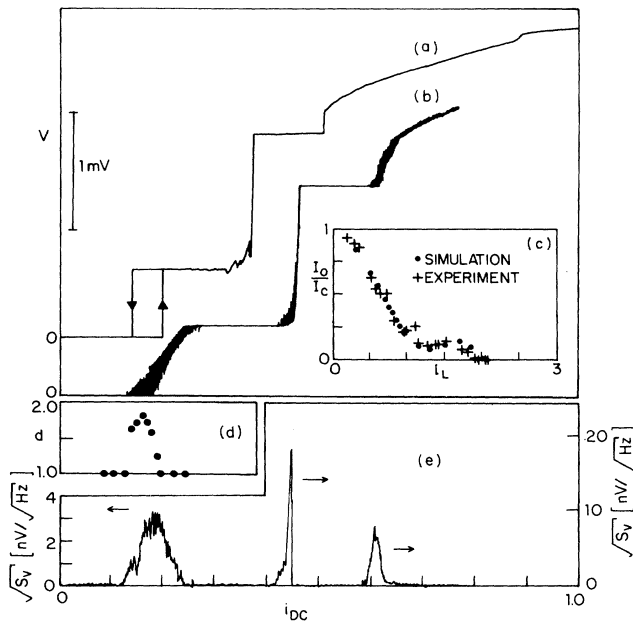


FIG. 1. (a) Simulated and (b) experimental  $I$ - $V$  curves. The three flat regions are the zeroth,  $\frac{2}{3}$ , and second Josephson step. No noise is added to the simulated curve. The hysteretic behavior in (a) is found if continuity in  $\phi$  and  $\dot{\phi}$  is maintained as  $i_{dc}$  is increased; random phase-space initial conditions can produce solutions on either step. (c) Dependence of the critical current of the junction on the laser drive. (d) Computed basin boundary dimension and (e) experimental noise power measurements at 10 kHz as a function of dc bias. Curves (a) and (b) and plots (d) and (e) are all for  $i_L = 1$  and share the same horizontal scale.

linear approximation for  $R$ .

After the calculation of the  $I$ - $V$  curves, the simulations were used to analyze the phase-space orbits of the system. In some "noisy" experimental regions, intrinsic chaotic motion was observed, characterized by orbits on a strange attractor (with  $i_N = 0$ ); we shall term such regimes type A. In other experimentally noisy regions, a fundamentally different behavior (type B) was observed in simulations; namely, all phase-space orbits found were periodic in the absence of added noise, each converging to a simple point attractor. Which attractor the system converged on, however, depended very sensitively on the initial values of  $\phi$  and  $\dot{\phi}$ . Despite the difference in the simulation, the low-frequency noise values observed experimentally for both type-A and type-B regions were comparable for the entire parameter region studied. The measured power spectrum (10 kHz–100 Hz) in both type-A and type-B regions was found to be approximately  $1/f$  from 10 Hz to 1 kHz; the dependence was more complicated at higher frequencies. For example, a large peak was found at  $\sim 5$  kHz, which cor-

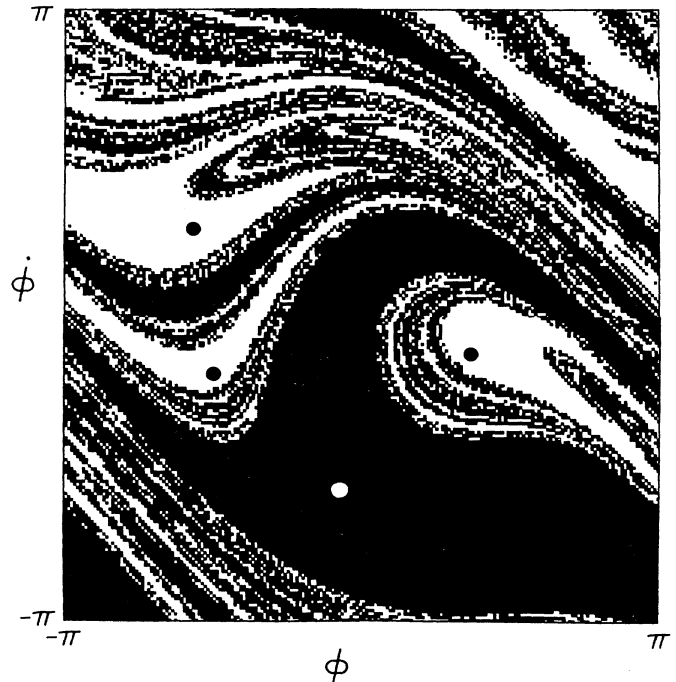


FIG. 2. Basins of attraction for  $i_L = 1$  and  $i_{dc} = 0.15$ . The white region is the basin of the  $\frac{2}{3}$ -step solution, corresponding to the three-point Poincaré section indicated by the centers of the black circles. The black region is the basin of the zeroth-step solution, with one-point Poincaré section (white circle). No noise is included.

responded to a small ( $\leq 0.01\%$ ) modulation in the laser power supply, indicating an extreme noise sensitivity of the device in these regions.

To gain a better understanding of the mechanism behind the high experimental noise values in the relatively unexplored type-B regions, we focused our simulations on one typical parameter range,  $i_L = 1$   $0.09 < i_{dc} < 0.25$ . With no added noise, dependent upon the initial conditions, one of two periodic solutions was found. The periodicity of these solutions was exact, within the accuracy of our simulations, over several thousands of drive cycles. The basins of attraction of these solutions, however, were found to be extremely complex, as illustrated in Fig. 2, by use of a  $200 \times 200$  grid of initial conditions. The RSJ equation (with  $i_N = 0$ ) was solved for each initial condition on the grid and, after an initial transient, the system would converge on one of two phase-locked solutions. If the system converged on the first, corresponding to a zeroth-step solution ( $\langle V \rangle = 0$ ), a black square was plotted. If the system converged on the second, corresponding to  $\langle V \rangle = \frac{2}{3}(\hbar\omega_L/2e)$ , the " $\frac{2}{3}$ " step, a white square was plotted. Thus, the black and white regions in Fig. 2 depict the two basins of attraction. The basin boundary has a fractal structure, of dimension

$d = 1.75$ , estimated by measurement of a correlation exponent, as described by Grassberger and Procaccia.<sup>12</sup>

Grebogi *et al.*<sup>9</sup> developed an argument relating the dimension of the basin boundary to the sensitivity of the system to initial conditions. They point out that if the initial conditions are uncertain by a small amount  $\epsilon$ , in  $D$ -dimensional phase space, the fraction of solutions starting close enough to the boundary to have an uncertain outcome is

$$f \sim \epsilon^{D-d}, \quad (2)$$

where  $d$  is the fractal dimension of the boundary. This predicts a large fraction of uncertain solutions and thus extraordinary sensitivity for  $d \sim D$ . Our simulations show a fractal basin boundary with large  $d$  for a significant range ( $\sim \pm 0.1$ ) of  $i_{dc}$  and laser current values, as shown for  $i_{dc}$  in Fig. 1(d). This regime should then exhibit very high sensitivity to uncertainty in initial conditions and, going one step further, to noise. Our experimental results back this hypothesis, as shown in Fig. 1(e). Displayed is the noise output measured on a PAR 124 lock-in amplifier in the ac voltmeter mode at 10 kHz with a 10% bandwidth. The variation in the experimental noise output in the region studied corresponds qualitatively to the variation of the calculated fractal basin boundary dimension with  $i_{dc}$ , as expected on the basis of the above argument, given thermal and shot-noise inputs in the experimental system. By contrast, the experimental variation with  $i_{dc}$  correlates less well, for example, with the nearly constant slope of the smoothed  $I$ - $V$  curve in this region. No values of  $d$  are shown in Fig. 1(d) for  $i_{dc} > 0.3$ , since no sensitive

dependence on initial conditions (i.e., no fractal basin boundary) was observed in the simulations. The two other noise peaks displayed (at  $i_{dc} \sim 0.45$  and  $\sim 0.62$ ) are associated with type-A intrinsic chaos and noise amplification due to high dynamic resistance of the  $I$ - $V$  curve.

Our basin-boundary study thus provides a mechanism to explain the high experimental noise values in the type-B regions. To obtain the phase-space motion of the system and a measure of the concomitant noise, we reverted to simulations. Noise was first included in the calculations as a white Johnson noise source.<sup>4</sup> Every simulation was begun with the system at a very high noise temperature ( $T \sim 1000$  K) and then gradually "annealed" until the desired temperature range was reached. After we waited for some additional cycles to discard initial transients, the Poincaré section and the power spectrum of the solution were calculated over at least 3200 cycles, with a time step of one-thousandth of a drive cycle.

The Poincaré section of Fig. 3(a) shows the behavior in a fractal basin boundary regime if only a small amount of noise ( $T = 1$  K) is added to the system. The motion is still essentially periodic and qualitatively similar to the case with no added noise, depicted in Fig. 2 by black circles; the orbit is still well within the basin of attraction of the  $\frac{2}{3}$  step. If we add more noise, the nature of the orbit becomes very different, as shown in Fig. 3(b). The resulting Poincaré section is stretched out anisotropically, reproducibly filling in a complicated region of phase space. It is very similar to the Poincaré section for an intrinsic chaotic regime (type A), displayed in Figs. 3(c) and 3(d). In general, we found a great similarity in all the Poincaré sections calculated for experimentally noisy regimes (types A

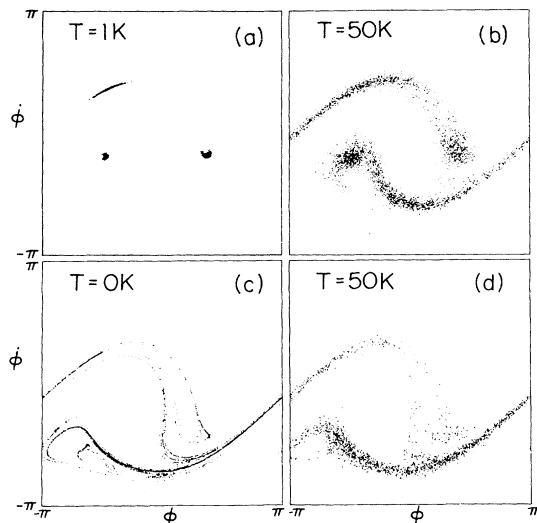


FIG. 3. Effect of added Johnson noise on the Poincaré sections for the system: (a), (b) in a fractal basin boundary regime at  $i_{dc} = 0.18$  and  $i_L = 1$ , and (c), (d) in an "intrinsic" chaotic regime at  $i_{dc} = 0.15$  and  $i_L = 1.5$ .

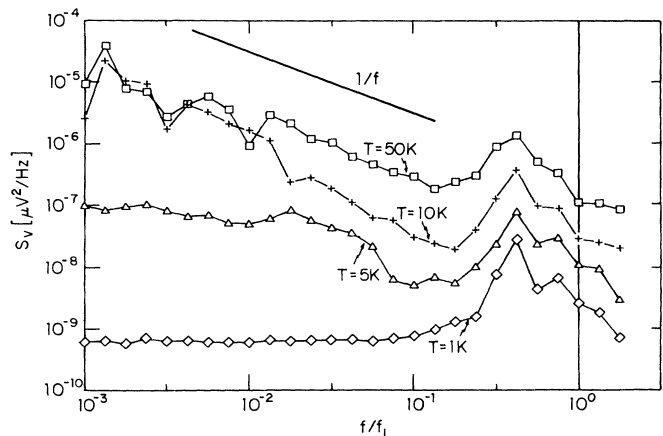


FIG. 4. Effect of added Johnson noise on the power spectra of the solutions in a fractal basin boundary regime. Parameters are  $i_{dc} = 0.18$ ,  $i_L = 1$ , and the effective temperature of the added noise varies from  $T = 1$  to  $T = 50$  K.

and B) as long as the effect of thermal noise ( $T > 5$  K) was included, providing a plausible explanation for the comparable noise values observed experimentally in type-A and type-B regions.

The power spectrum of the solutions in the fractal basin boundary regime show noise-induced intermittency leading to large low-frequency noise. This is shown in Fig. 4 where the spectrum is approximately  $1/f$  for at least two frequency decades over a wide noise temperature range. (The peak at  $f_L/3$  reflects the residual effect of the period-three phase lock.) Such behavior is common in the parameter region investigated here. The occurrence of switching and excess low-frequency noise has a well-defined threshold noise temperature. The Poincaré section for 5 K is still localized within the basin of attraction of the  $\frac{2}{3}$ -step solution but comes very close to the boundary. A small increase in the added noise pushes the orbit out into the basin boundary. This causes sudden changes in the Poincaré section, which begins to resemble a strange attractor, and in the power spectrum of the solution, which develops excess low-frequency noise. The situation is qualitatively similar to an interior crisis<sup>9</sup> occurring in intrinsic chaotic systems, in the neighborhood of which an intrinsic approximately  $1/f$  power spectrum was recently found by Gwinn and Westervelt.<sup>6</sup>

If shot noise is included in the calculation,<sup>11</sup> similar results are obtained. However, the  $1/f$  power spectrum now holds down to  $T=0$ , since the magnitude of the added noise bottoms out at a finite value, corresponding to a Johnson noise temperature of the order of 10 K, as a result of the varying instantaneous voltage across the junction. In contrast with the classical pendulum model, here the *quantization* of the *electronic charge* induces shot noise in the junction current sufficient enough to destroy the system's periodic motion and induce excess low-frequency noise, even at  $T=0$ .

In conclusion, we have shown how the presence of a fractal basin boundary in the dynamics of a nonlinear system may give rise to chaotic motion and extraordinary low-frequency noise when the effect of naturally occurring thermal and shot noise is included. Both the nature of the motion and the magnitude of the mea-

sured noise output are comparable to those found in intrinsic chaotic regimes.

We are pleased to acknowledge some essential suggestions by E. G. Gwinn and helpful discussions with S. W. Teitsworth, R. F. Voss, and J. U. Free. We also acknowledge the contribution of the samples by L. N. Smith, use of computer equipment by S. L. Pope, and the collaboration of J. U. Free in computations at Eastern Nazarene College. This research was supported in part by the U.S. Office of Naval Research under Contract No. N00014-83-K-0383 and by the Joint Services Electronics Program under Contract No. N00014-84-K-0465.

<sup>1</sup>B. A. Huberman, J. P. Crutchfield, and N. H. Packard, *Appl. Phys. Lett.* **37**, 750 (1980).

<sup>2</sup>R. L. Kautz, *J. Appl. Phys.* **52**, 3528 (1981), and **58**, 424 (1985).

<sup>3</sup>R. F. Miracky, J. Clarke, and R. H. Koch, *Phys. Rev. Lett.* **50**, 856 (1983); R. F. Miracky, M. H. Devoret, and J. Clarke, *Phys. Rev. A* **31**, 2509 (1985).

<sup>4</sup>M. Octavio, *Phys. Rev. B* **29**, 1231 (1984); M. Octavio and C. R. Nasser, *Phys. Rev. B* **30**, 1586 (1984).

<sup>5</sup>N. F. Pedersen and A. Davidson, *Appl. Phys. Lett.* **39**, 830 (1981); D. C. Cronemeyer, C. C. Chi, A. Davidson, and N. F. Pedersen, *Phys. Rev. B* **31**, 2667 (1985).

<sup>6</sup>E. G. Gwinn and R. M. Westervelt, *Phys. Rev. Lett.* **54**, 1613 (1985).

<sup>7</sup>Qing Hu, J. U. Free, M. Iansiti, O. Liengme, and M. Tinkham, *IEEE Trans. Magn.* **21**, 590 (1985).

<sup>8</sup>M. J. Kajanto and M. M. Salomaa, *Solid State Commun.* **53**, 99 (1985).

<sup>9</sup>C. Grebogi, S. W. McDonald, E. Ott, and J. A. Yorke, *Phys. Lett.* **99A**, 415 (1983); C. Grebogi, E. Ott, and J. A. Yorke, *Physica (Amsterdam)* **7D**, 181 (1983).

<sup>10</sup>H. Kroger, L. N. Smith, and D. W. Jillie, *Appl. Phys. Lett.* **39**, 280 (1981).

<sup>11</sup>W. C. Danchi, F. Habbal, and M. Tinkham, *Appl. Phys. Lett.* **41**, 883 (1982); W. C. Danchi, J. Bindslev Hansen, M. Octavio, F. Habbal, and M. Tinkham, *Phys. Rev. B* **30**, 2503 (1984).

<sup>12</sup>P. Grassberger and I. Procaccia, *Phys. Rev. Lett.* **50**, 346 (1983).